Network effects and pathways in deep brain stimulation in Parkinson's disease

Nabin Koirala, Vinzenz Fleischer, Oliver Granert, Günther Deuschl, Muthuraman Muthuraman, Sergiu Groppa

Network effects and pathways in Deep brain stimulation in Parkinson's disease*

Koirala N, Fleischer V, Granert O, Deuschl G, Muthuraman M, Groppa S

Abstract— Deep brain stimulation of subthalamic nucleus (STN-DBS) became a standard therapeutic option in Parkinson's disease (PD), even though the underlying modulated network of STN-DBS is still poorly described. Probabilistic tractography and connectivity analysis as derived from diffusion tensor imaging (DTI) were performed together with modelling of implanted electrode positions and linked postoperative clinical outcome. Fifteen patients with idiopathic PD without dementia were selected for DBS treatment. After pre-processing, probabilistic tractography was run from cortical and subcortical seeds of the hypothesized network to targets represented by the positions of the active DBS contacts. The performed analysis showed that the projections of the stimulation site to supplementary motor area (SMA) and primary motor cortex (M1) are mainly involved in the network effects of STN-DBS. An involvement of the "hyperdirected pathway" and a clear delimitation of the cortico-spinal tract were demonstrated. This study shows the effects of STN-DBS in PD distinctly rely on the network connections of the stimulated region to M1 and SMA, motor and premotor regions.

I. INTRODUCTION

High-frequency deep brain stimulation of the subthalamic nucleus (STN-DBS) is an effective therapy option for patients with Parkinson's disease (PD) [1]. The effect on major clinical motor symptoms as tremor, rigidity, and bradykinesia is unequivocal. Furthermore DBS improve non-motor symptoms of the disease, possibly through its network effects [2]. Despite the clinical success of DBS, its mechanisms at the local and systemic level have not been fully elucidated. Furthermore there is no clear data on the anatomical structures targeted. A complex modulation of the basal ganglia loops or the cortico-subcortical networks is hypothesised [3]. Early studies attested that high-frequency stimulation might modulate the neuronal activity within the STN [4]. However, DBS presumably does not only change the neural activity in the nuclei but furthermore targets the fibre tracts entering, exiting, or passing the stimulation site [5]. Moreover an interaction with the pathological oscillations in distinct brain networks might be a critical feature of the DBS induced clinical response in PD [7, 8].

Studies on primates and recent studies on humans attested the existence of the so-called hyperdirect cortical STN projections [6]. Furthermore this pathway might be of special importance for the effects of STN-DBS [7].

Here we analyse the connections of the electrode regions by the use of diffusion tensor imaging (DTI) and probabilistic tractography. Therefore we focus on cortical and subcortical projection to the electrode site that might be involved in the clinical effect of STN-DBS. We hypothesise that these connections play an important role for STN-DBS and their characteristics are crucial for the clinical outcome and stimulation parameters. Furthermore we consider the connectivity data as possible predictors that relate to postoperative clinical outcome scores such as UPDRS-III (UPDRS – motor score) or stimulation parameters for an optimal clinical response.

II. METHODS

A. Data Acquisition

Fifteen patients with idiopathic PD without dementia selected for DBS treatment (11 males, age 63.3±8.2, Hoehn and Yahr 3.5±0.8) selected for DBS treatment were randomly included in this study. All patients received, after clinical and neuropsychological assessment, bilateral STN electrodes. The UPDRS-III values in the medication OFF, stimulation ON state have been used to calculate the quotient to the preoperative UPDRS-III score in medication ON state (mentioned further as qUPDRS) have been selected for the parameter of clinical outcome and included into further analysis. The surgical procedure has been previously described in detail [8]. The study protocol used was approved by the local ethics committee and all patients have signed a written consent regarding the procedure.

All patients underwent a preoperative high resolution MRI (3T) using an 8-channel SENSE head coil. We acquired diffusion sensitive MRI of the whole brain at 2 mm isometric voxel resolution covering a field of view of 224 x 224 mm. DTI included three acquisitions of 32 gradient directions plus 5 b0 images for each acquisition (b value 1000 s/mm^2, TE = 59 ms, TR = 11855 ms, fat saturation "on", 60 contiguous slices). Moreover we obtained a high-resolution T1-weighted structural image of the whole brain using a standard MPRAGE sequence (TR = 7.7 ms, TE = 3.6 ms, flip angle = 8°). The T1-scan consisted of 160 contiguous sagittal slices with 1 mm isometric voxels and a field of view = 240 x 240 mm. On the first postoperative day a further recording was performed on a 1.5 T scanner with a protocol consisting of a T1-weighted structural image of the whole

brain using a standard MPRAGE sequence (TR = 10.7 ms, TE = 1.96 ms, flip angle = 8°). The structural brain scan consisted of 160 contiguous coronal slices with 2 mm isometric voxel size and a field of view = 256 x 256 mm.

B. Preprocessing

Electrode positions and electrode trajectory were determined by performing the following image analysis procedure:

First step: Post-operative T1 images were used to determine the position of the electrode lead. The lead was mathematically modelled by a straight line and the position was determined from a set of manually placed 3D space points (markers) along the electrode trajectory. The electrode trajectory was determined within the MRI T1 weighted images using all three orthogonal views (sagittal, coronal and transversal). Markers were placed at the target points, near the points of exit and uniformly along the trajectory artefact. Finally, a three dimensional least square optimization procedure was used to determine the exact position of the trajectory. Based on the optimized lead position the T1 intensity profile was extracted along the trajectory. The exact electrode positions were then determined by shifting the four contacts manually along the lead such that the center of the intensity dip, apparent in the extracted intensity profile, was in correspondence with the lead contacts.

Second step: Geometrically determined electrode contact positions were used to create spatially Gaussian weighting masks. The masks were calculated by specifying the following two standard deviations: I. along the lead to model contact dimensions, known from manufacturer's annotations; II. in orthogonal directions to model stimulation depth. The multivariate Gaussians were centered at the contact positions determined as described in the first step. We restricted our analysis to a mask with an extension of two standard deviations along the lead and two standard deviations in depth (isometric mask with 4.7 mm full width at half maximum (FWHM), corresponding to a radius of ~2.4 mm). These parameters were selected considering existing literature that attests that neural elements up to a distance of 2 mm from the active contact might be excited by DBS [9]. The generated Gaussian masks were then used for further analysis. To allow bias-free definition of seed and target areas unaffected by subjective judgments about anatomical correspondences, we built masks for cortical seeds from anatomical coordinates known from a meta-analysis for activation studies [10]. The generated masks were spheres with a radius of 5 mm centered at the following MNI coordinates: primary motor cortex [M1 (-37 -21 58)], dorsal and ventral premotor cortex [PMd (-30 -4 58), PMv (-50 5 22)] and SMA (-2 -7 55) [11]. The coordinates were transformed into MNI space using GingerALE [12]. ROIs of Globus Pallidus internus (GPi) and Globus Pallidus externus (GPe) were generated from the MNI probability atlas by including the entire areas [13].

C. Tractography analysis

The aim of our tractography analysis was to generate voxel-based connectivity index maps in the regions of the DBS electrodes. We used all voxels in the basal ganglia and the midbrain structures as generated by the MNI atlas and defined this area as target region [14]. A multi-fiber model was fit to the diffusion data at each voxel, allowing for tracing through regions of crossing fibers [15]. Here, we drew 5,000 streamline samples from our seed voxels to form an estimate of the probability distribution of connections from each seed voxel using FSL (v 4.1). Tracts generated are volumes wherein values at each voxel represent the number of samples (or streamlines) that passed through that voxel. For the elimination of spurious connections, tractography in individual subjects was restricted to include only voxels through which at least 10 percent of all streamline samples had passed [16]. The probability of connection to the target mask was obtained from the proportion of samples that reached each of the voxels. The individual maps were then normalized to calculate a tract probability at each voxel of the target region for each tract and subject. This connectivity values were then extracted from the Gaussian masks and feed into further analysis. Further we performed another tractography analysis to generate a voxel-based connectivity index map to delimitate the cortical connections to the electrode regions from the cortico-spinal tract. The analyzed tract started as well from the M1-mask but passed a conjunction mask of the ipsilateral cerebral peduncle region and internal capsule [17]. The connectivity values of the electrode regions have been then extracted as described above.

D. Statistical analysis

The correlation analysis was performed using SPSS software (Version 16.0, SPSS Inc, Chicago, IL, USA). To improve the statistical power of the data analysis, we pooled the data from both sides. Stimulation intensity amplitudes and the quotient of the post- to preoperative UPDRS-III (qUPDRS) were introduced into further analysis of covariance (ANCOVA). T-test has been calculated for the clinical outcome measurements. For the cortico-spinal tractography analysis, we calculated two single linear regression analyses with the connectivity data from the cortico-spinal tract and "DBS intensity" and "qUPDRS"-values.

III. RESULTS

A. Tractography analysis

The analysis of covariance (ANCOVA) including the continuous factor DBS stimulation intensity revealed a significant main effect for the factor Seed [F(5, 140)=2.35, p<0.05]. The interaction between the factors Seed and DBS intensity was also significant [F(5, 140)=2.30, p<0.05]. Model correlation with the continuous factor DBS intensity

was significant for the variables of connectivity indices from M1 (r=0.45, F=7.30, p<0.05) and SMA (r=0.39, F=5.28, p<0.05, Figure 1A & 1B).
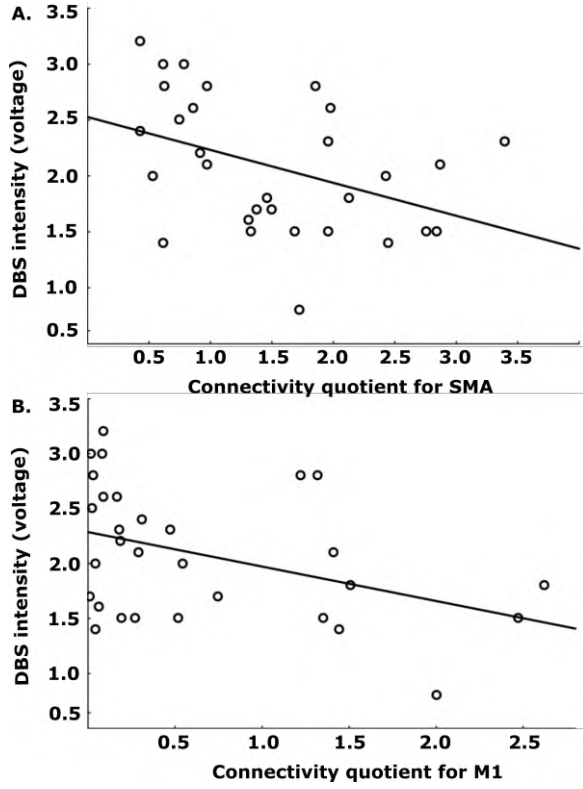

Figure 1.   Correlation analysis of connectivity ratios for M1 (A) and SMA (B) to stimulation intensity at the active contact.

The ANCOVA including the continuous factor qUPDRS revealed a significant main effect for the factor Seed [F(5, 140=8.81, p<0.05] but showed no other significant interactions between terms. No correlations with connectivity values from other cortical (PMd, PMv) or subcortical seeds (GPi or GPe) achieved statistical significance in the above mentioned analyses.

B. Delimitation of the cortico-spinal tract

The two linear regression analyses for the connectivity values from the cortico-spinal tract and "DBS intensity" (t=-1.2, p>0.1) and "qUPDRS" (t=-0.4, p>0.1) were not significant. On the visual inspection of the tract probability maps and VTA (volume tissue activation) positions, the corticospinal tract was positioned more laterally, while for electrodes localised in the neighbourhood of the cortico-spinal tract lower stimulation intensities have been chosen, possibly to reduce the effects (Figure 2).
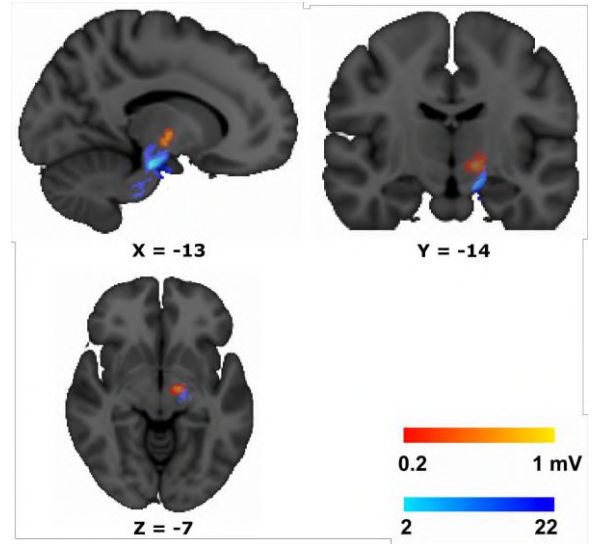

Figure 2.   Probabilistic tractography results with schematic presentation of the binarized cortico-spinal tract (blue) and electrode region. Color bar: connectivity values represent the number of subjects with positive voxels and current intensity at the effective electrode.

IV. DISCUSSION

Using diffusion MRI, we show that the connectivity pattern as derived from probabilistic tractography from M1 and SMA directly correlate with the applied voltage at the active contact for an optimal clinical effect after STN-DBS. The connectivity profile from these two cortical regions might become important predictors for STN-DBS. The main purpose of this study was to reconstruct the anatomical network modulated by STN-DBS. So far little is known about the systemic mechanisms of the STN-DBS. Important data on possible network interactions was obtained from animal studies, while direct translations to human models are lacking [18].

The direct involvement and imperative role of the primary motor cortex for the effects of the STN-DBS have been demonstrated in two recent studies. They showed that DBS induced antidromic spikes in Layer V pyramidal cells triggered a dampened oscillation of local field potentials in cortex with a resonant frequency around 120 Hz [19]. With optogenetics and solid-state optics a direct activation of cortical afferents from M1 projecting to the STN region was observed and an explicitly associated with therapeutic benefit was determined [20]. Seminal data on the role of the motor cortex for the effects of the STN-DBS provided a study on Parkinsonian rats, that showed that the corrective action is upon the cortex, where stochastic antidromic spikes originating from the STN directly modify the firing probability of the corticofugal projection neurons, destroy the dominance of beta rhythm [7]. In summary these studies together with our probabilistic and structural data suggest that STN-DBS specifically modulates the M1-STN and SMA-STN connections via either the hyperdirect pathway or possible loops, functionally related circuits in a way that normalise the overall cortico-basal-ganglia-cortical network and the circulating pathological activity.

In our view, the correlative evidence of the stimulation parameters and connectivity values explains the fiber tract integrity and the associated modifiability profile of the connection to the motor and premotor areas through STN-DBS. Our results are supported by existing effective connectivity data too, showing an increased cortical output to STN via hyperdirect tract area in the Parkinsonian primates compared to the control group [21]. Stronger structural connectivity in these circuits might be further the basis for the oscillations that have to be counteracted by STN-DBS.

An important point for the discussion of STN-DBS effects in the light of these results is the possible direct activation of the pyramidal tract fibers that might worsen bradykinesia and akinesia and negatively influence the clinical outcome [22]. Since both regions M1 and SMA present wide corticospinal projections the importance of these for the effects of STN-DBS could not be completely ruled out. Nonetheless the adjacent studied premotor cortical areas (PMd and PMv) are similarly to M1 and SMA sources for dense corticospinal projections [23]. The connectivity analysis of these regions to the electrode sites did not depict any correlative relationships. Furthermore a direct stimulation of the pyramidal tract would activate cranial or spinal motoneurons and lead to muscle contractions, which was not the case in all of our patients as well. The performed analysis of the connectivity data of the generated cortico-spinal tract and the lack of the correlation to the stimulation parameters or clinical outcome make the direct involvement of this pathway for the STN-DBS effects.

V. CONCLUSION

In conclusion our data suggests that the effects of STN-DBS in PD distinctly depend on the network connections of the stimulated region to M1 and SMA, motor and premotor regions. We observed no correlations with connectivity values from other cortical (PMd, PMv) or subcortical seeds (GPi or GPe). Furthermore we witnessed DTI and probabilistic tractography as the important tools that can be used to refine STN-DBS targeting and better elucidate the achieved systemic effects.

REFERENCES

[1] G. Deuschl, C. Schade-Brittinger, P. Krack, J. Volkmann, H. Schafer, K. Botzel, *et al.*, "A randomized trial of deep-brain stimulation for Parkinson's disease," *New England Journal of Medicine,* vol. 355, pp. 896-908, Aug 31 2006.

[2] C. C. McIntyre and P. J. Hahn, "Network Perspectives on the Mechanisms of Deep Brain Stimulation," *Neurobiol Dis,* vol. 38, pp. 329-37, Jun 2010.

[3] C. C. McIntyre and P. J. Hahn, "Network perspectives on the mechanisms of deep brain stimulation," *Neurobiol Dis,* vol. 38, pp. 329-337, 2010.

[4] L. Garcia, J. Audin, G. D'Alessandro, B. Bioulac, and C. Hammond, "Dual Effect of High-Frequency Stimulation on Subthalamic Neuron Activity," *The Journal of Neuroscience,* vol. 23, pp. 8743-8751, September 24, 2003 2003.

[5] V. Gradinaru, M. Mogri, K. R. Thompson, J. M. Henderson, and K. Deisseroth, "Optical deconstruction of parkinsonian neural circuitry," *Science,* vol. 324, pp. 354-9, Apr 17 2009.

[6] A. Nambu, H. Tokuno, and M. Takada, "Functional significance of the cortico-subthalamo-pallidal [] hyperdirect'pathway," *Neuroscience Research,* vol. 43, pp. 111-117, 2002.

[7] Q. Li, Y. Ke, Danny C. W. Chan, Z.-M. Qian, Ken K. L. Yung, H. Ko, *et al.*, "Therapeutic Deep Brain Stimulation in Parkinsonian Rats Directly Influences Motor Cortex," *Neuron,* vol. 76, pp. 1030-1041, 12/6/ 2012.

[8] B. Schrader, W. Hamel, D. Weinert, and H. M. Mehdorn, "Documentation of electrode localization," *Mov Disord,* vol. 17 Suppl 3, pp. S167-74, 2002.

[9] J. B. Ranck, "Which elements are excited in electrical stimulation of mammalian central nervous system: a review," *Brain Research,* vol. 98, pp. 417-440, 1975.

[10] M. A. Mayka, D. M. Corcos, S. E. Leurgans, and D. E. Vaillancourt, "Three-dimensional locations and boundaries of motor and premotor cortices as defined by functional brain imaging: A meta-analysis," *NeuroImage,* vol. 31, pp. 1453-1474, 2006.

[11] M. Argyelan, M. Carbon, M. Niethammer, A. M. Ulug, H. U. Voss, S. B. Bressman, *et al.*, "Cerebellothalamocortical connectivity regulates penetrance in dystonia," *J Neurosci,* vol. 29, pp. 9740-9747, 2009.

[12] S. B. Eickhoff, A. R. Laird, C. Grefkes, L. E. Wang, K. Zilles, and P. T. Fox, "Coordinate-based ALE meta-analysis of neuroimaging data: A random-effects approach based on empirical estimates of spatial uncertainty," *Human Brain Mapping,* vol. 30, p. 2907, 2009.

[13] J. Mazziotta, A. Toga, A. Evans, P. Fox, and J. Lancaster, "A probabilistic atlas of the human brain: theory and rationale for its development the international consortium for brain mapping (ICBM)," *NeuroImage,* vol. 2, pp. 89-101, 1995.

[14] J. L. Lancaster, M. G. Woldorff, L. M. Parsons, M. Liotti, C. S. Freitas, L. Rainey, *et al.*, "Automated Talairach atlas labels for functional brain mapping," *Hum Brain Mapp,* vol. 10, pp. 120-131, 2000.

[15] T. Behrens, H. J. Berg, S. Jbabdi, M. Rushworth, and M. Woolrich, "Probabilistic diffusion tractography with multiple fibre orientations: What can we gain?," *Neuroimage,* vol. 34, pp. 144-155, 2007.

[16] E. D. Boorman, J. O'Shea, C. Sebastian, M. F. S. Rushworth, and H. Johansen-Berg, "Individual differences in white-matter microstructure reflect variation in functional connectivity during choice.," *Curr Biol,* vol. 17, pp. 1426-1431, 2007/08/21 2007.

[17] S. Jbabdi, M. W. Woolrich, J. L. R. Andersson, and T. E. J. Behrens, "A Bayesian framework for global tractography," *Neuroimage,* vol. 37, pp. 116-129, 2007.

[18] T. Hershey, F. J. Revilla, A. R. Wernle, L. McGee-Minnich, J. V. Antenor, T. O. Videen, *et al.*, "Cortical and subcortical blood flow effects of subthalamic nucleus stimulation in PD," *Neurology,* vol. 61, pp. 816-21, Sep 23 2003.

[19] Q. Li, Y. Ke, D. C. W. Chan, Z. M. Qian, K. K. L. Yung, H. Ko, *et al.*, "Therapeutic Deep Brain Stimulation in Parkinsonian Rats Directly Influences Motor Cortex," *Neuron,* vol. 76, pp. 1030-1041, 2012.

[20] V. Gradinaru, M. Mogri, K. R. Thompson, J. M. Henderson, and K. Deisseroth, "Optical Deconstruction of Parkinsonian Neural Circuitry," *Science,* vol. 324, pp. 354-359, April 17, 2009 2009.

[21] A. Moran, E. Stein, H. Tischler, and I. Bar-Gad, "Decoupling neuronal oscillations during subthalamic nucleus stimulation in the parkinsonian primate," *Neurobiology of Disease,* vol. 45, pp. 583-90, Jan 2012.

[22] W. Xu, S. Miocinovic, J. Zhang, K. B. Baker, C. C. McIntyre, and J. L. Vitek, "Dissociation of motor symptoms during deep brain stimulation of the subthalamic nucleus in the region of the internal capsule," *Experimental Neurology,* vol. 228, pp. 294-7, Apr 2011.

[23] H. Tokuno and A. Nambu, "Organization of nonprimary motor cortical inputs on pyramidal and nonpyramidal tract neurons of primary motor cortex: An electrophysiological study in the macaque monkey.," *Cereb Cortex,* vol. 10, pp. 58-68, 2000/01/ 2000.